The Interface of the Most Polar Layered Oxide Superconductor Solved by Coordinated Experiments and Theory

Berit H. Goodge[1,2], Benjamin Geisler[3], Kyuho Lee[4,5], Motoki Osada[4,6], Bai Yang Wang[4,5], Danfeng Li[4,7], Harold Y. Hwang[4,8], Rossitza Pentcheva[3] and Lena F. Kourkoutis[1,2]

[1.] School of Applied and Engineering Physics, Cornell University, Ithaca, NY, USA.
[2.] Kavli Institute at Cornell for Nanoscale Science, Cornell University, Ithaca, NY, USA.
[3.] Department of Physics and Center for Nanointegration (CENIDE), University of Duisburg-Essen, Duisburg, Germany.
[4.] Stanford Institute for Materials and Energy Sciences, SLAC National Accelerator Laboratory, Menlo Park, CA, USA.
[5.] Department of Physics, Stanford University, Stanford, CA, USA.
[6.] Department of Materials Science and Engineering, Stanford University, Stanford, CA, USA.
[7.] Department of Physics, City University of Hong Kong, Kowloon, Hong Kong, China.
[8.] Department of Applied Physics, Stanford University, Stanford, CA, USA.

The recently discovered nickel-based oxide superconductors [1] provide a close analogue and long-sought opportunity for experimental comparison to the high-T_c cuprates. Despite their nominally isostructural infinite-layer forms and isoelectronic metal $3d^9$ configurations, however, several key distinctions between the two systems have been observed, including differences in the hybridization, charge-transfer energy, and pairing mechanism [2-4]. Additionally, the nickelates present by far the most polar layered oxide superconductor yet discovered, with strongly charged R^{3+} and $Ni^{1+}O^{2-}_2$ atomic planes. Furthermore, thus far superconducting thin films have only been demonstrated grown epitaxially on stabilizing substrates such as $SrTiO_3$, compounding this inherent polarity with a large polar discontinuity at the atomic interface. The nature of this atomic interface presents important questions for understanding the phenomena observed in these films: for example, it has been predicted that an ideal interface between $NdNiO_2$ and $SrTiO_3$ may host a two-dimensional electron gas (2DEG) [5] with carrier density even higher than the superconducting $LaAlO_3$-$SrTiO_3$ polar interface [6].

With the ability to study buried interfaces with both high spatial and energy resolution, scanning transmission electron microscopy (STEM) and electron energy loss spectroscopy (EELS) offer the ideal platform to investigate such effects with both structural and chemical sensitivity. Here, we leverage atomic-resolution STEM-EELS to directly probe the electronic nature of the interface between infinite-layer nickelate thin films and $SrTiO_3$ substrate. Elemental mapping reveals the formation of a previously unpredicted single intermediate $Nd(Ti,Ni)O_3$ atomic layer which forms between the substrate and film. Figure 1a shows an example of this layer as observed in an undoped $NdNiO_2$ film on $SrTiO_3$, but the same effect has been observed across all films studied so far, irrespective of electron doping via chemical (Sr) substitution or cation species (Nd, Pr, La). Detailed measurements of the electronic structure across this interface were carried out on an aberration-corrected Nion UltraSTEM equipped with Quefina 2 camera, operating at a primary voltage of 100 kV with a modest probe current of ~13 pA to avoid beam-induced damage. Several line profiles across the interface were aligned and summed to produce high signal-to-noise-ratio EEL spectra suitable for analysis of subtle ELNES changes at each atomic layer, shown in Figure 1b and 1c. Atomic layers are indexed from the intermediate $(Ti,Ni)O_2$ plane (marked by the white triangle in Figure 1a), with indices increasing by positive (negative) integers progressing into the film (substrate). Note that the spectra in Figure 1b and 1c cascade opposite to the

film orientation shown in Figure 1a (i.e., substrate to film runs top to bottom) for clarity of display. Each spectrum is plotted with a bulk reference shown in grey: Ti-$L_{2,3}$ spectra are referenced to identical measurements of the $SrTiO_3$ substrate (far from the interface) and the O-K spectra are referenced to a best-fit linear combination of bulk-like references of $SrTiO_3$ and $NdNiO_2$ (far from the interface).

The Ti-$L_{2,3}$ edge shows only a minor filling between the e_g and t_{2g} peaks at the intermediate layer 0, but does not suggest significant modifications towards Ti^{3+} or other formal valence states. Instead, the subtle modification observed likely reflects changes to the coordination environment at the interface layer induced by the A-site cation (Nd vs. Sr) and partial Ni occupancy. The O-K edge, by comparison, shows more notable deviation from the generated reference spectra at layers near the interface. The broadening and shift of peak 'B' in layers -1 to 1 reflect the changing cation [7], while the evolution of the pre-peak feature 'A' can be used to track the oxygen filling in each unit cell [4], revealing a nominally complete transition to the 'reduced' infinite-layer structure at layer 1 in the film.

To more completely resolve the full interface atomic and electronic structure, we combine precise atomic structure analysis by HAADF-STEM imaging with density functional theory with Hubbard U term (DFT+U) calculations considering varying stoichiometry of the intermediate $Nd(Ti,Ni)O_3$ layer. The c-axis lattice distance is measured for each unit cell across the interface between consecutive A-site planes as shown by the dotted white bracket in the left panel of Figure 2a. A comparison between the experimental measurements and results of DFT+U calculations show clearly improved agreement when ~50% Ni occupancy is included in the intermediate layer as indicated by the arrows in the right panel of Figure 2a. The resolved atomic structure is presented in Figure 2b with the layer-resolved densities of states (DOS) in Figure 2c. With Ni present in the intermediate layer, the induced Jahn-Teller-like distortions "absorb" excess charge in the Ni $3d$ states (the grey states in layer 0) at the interface, effectively quenching the formation of a 2DEG in the $SrTiO_3$.

Together, the combination of atomic-resolution STEM-EELS and DFT+U calculations uncover the various structural effects at this unique, strongly polar interface and disentangle their contributions for alleviating the polar discontinuity [8, 9].
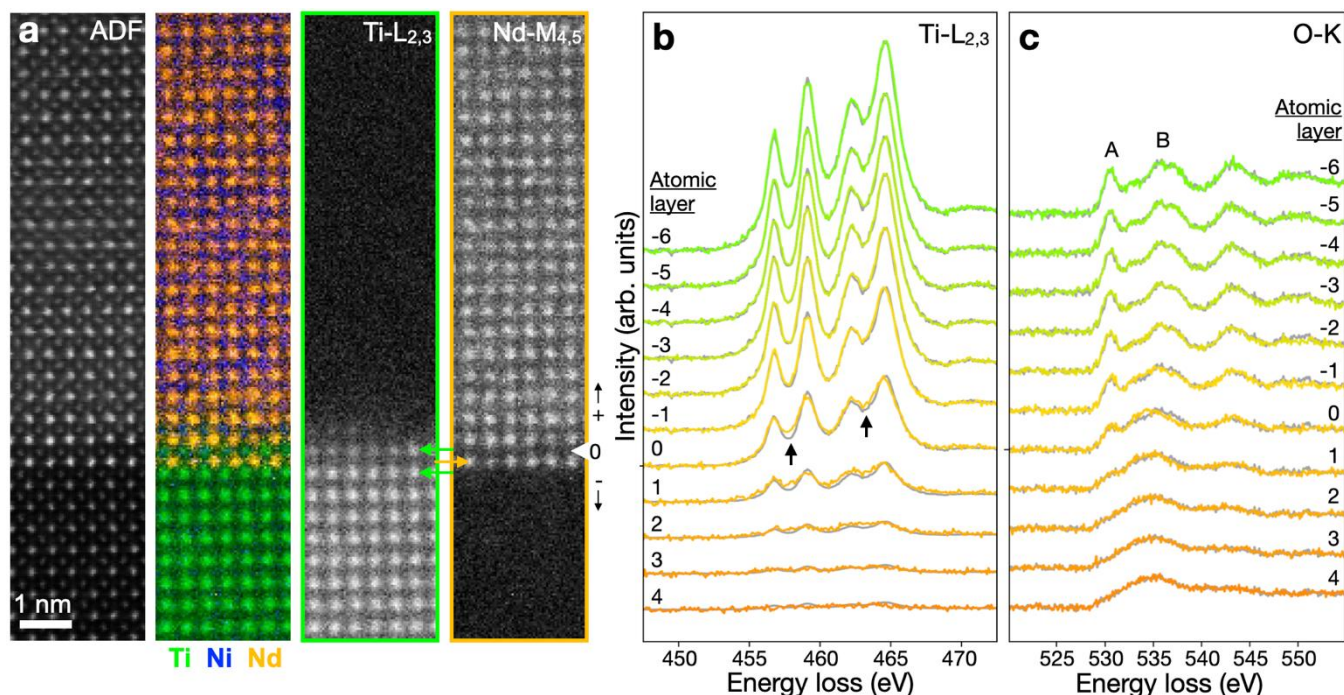
Figure 1. Cross-sectional elemental and chemical analysis by STEM-EELS offers insights to the strongly polar interface between $SrTiO_3$ and $NdNiO_2$ which are hidden to other spectroscopic methods. (a) Elemental mapping by atomic-resolution STEM-EELS reveals the formation of a single $Nd(Ti,Ni)O_3$ layer at the interface between the $SrTiO_3$ substrate and an infinite-layer $NdNiO_2$ thin film. ELNES analysis at each atomic layer across the interface of (b) the Ti-$L_{2,3}$ edge shows only subtle variations most likely due to the changes in coordination due to variations in cation stoichiometry, while (c) the O-K edge tracks not only the progression in cation species from Sr to Nd but also the oxygen occupancy in each atomic layer.
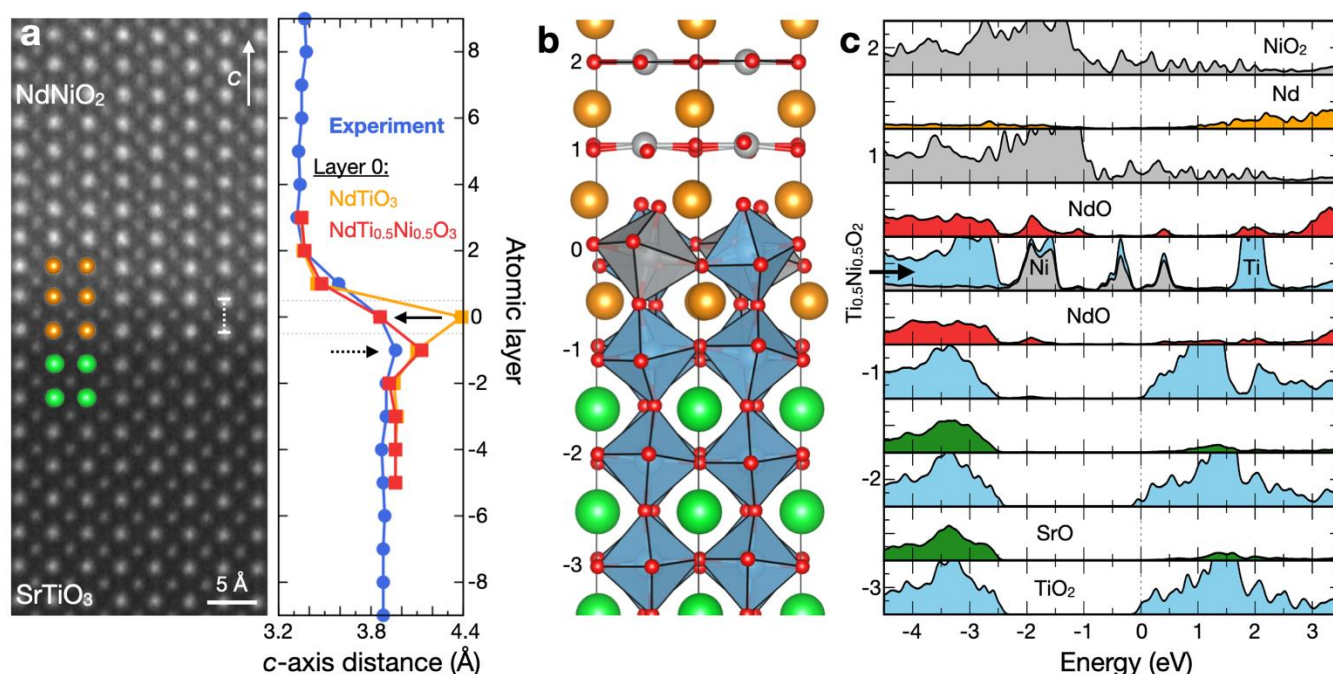
Figure 2. HAADF-STEM measurements combined with the STEM-EELS results shown in Fig. 1 provide validation for DFT+U models which predict the full atomic and electronic structure at each layer. (a) Experimental measurements of the c-axis distance across the interface are compared with DFT+U results for a pure $NdTiO_3$ intermediate layer and a mixed $NdTi_{0.5}Ni_{0.5}O_3$ intermediate layer. (b) DFT+U atomic model including a mixed intermediate layer shows how the presence of Ni allows Jahn-Teller-like distortions to accommodate excess charge. (c) The layer-resolved DOS calculated by DFT+U shows how the Ni $3d$ states (grey states at layer 0) help to effectively quench the formation of a 2DEG in the $SrTiO_3$ in agreement with the STEM-EELS results.

References:

[1] Li, et al. Nature **572**, 624 (2019).
[2] Gu, et al. Nat. Comm. **11**, 6027 (2020).
[3] Hepting, et al. Nat. Mater. **19**, 381 (2020).
[4] Goodge, et al. PNAS **118**, e2007683118 (2021).
[5] Geisler & Pentcheva. Phys. Rev. B **102**, 020502 (2020).
[6] Ohtomo & Hwang. Nature **427**, 423 (2004).
[7] Kourkoutis, et al. Phil. Mag. **90**, 4731 (2010).
[8] Goodge, et al. arXiv: 2201.03613 (2022).
[9] Supported by DOD AFOSR (FA 9550-16-1-0305), NSF (DMR-1719875), DOE BES MSD (DE-AC02-76SF00515), the Moore Foundation (GBMF9072), the Packard Foundation, and the German Research Foundation (DFG) within CRC/TRR 80 (Projects G3, G8) with computational time at magnitUDE granted by the Center for Computational Sciences and Simulation of the University of Duisburg-Essen (DFG grant nos. INST 20876/209-1 FUGG).